9

Permanent magnets

Permanent magnets are ferromagnetic materials that retain significant magnetization after the magnetizing current is removed.[1] In applications where space is constrained, permanent magnets can provide stronger fields than electromagnets, require no power source, and do not need cooling. After discussing the properties of bar magnets and magnetic circuits, we consider some models of the properties of magnets made from rare earth compounds. We conclude with a discussion of assemblies of permanent magnets, which can be used to produce desired multipole fields.

9.1 Bar magnets

Let us consider a cylindrical sample of permanent magnet material with uniform magnetization M along the axis of the cylinder, as shown in Figure 9.1. Recall from Equation 3.23 that the vector potential can be written as

$$\overrightarrow{A} = \frac{\mu_0}{4\pi}\int \frac{\overrightarrow{M} \times \hat{n}}{R}\, dS + \frac{\mu_0}{4\pi}\int \frac{\nabla \times \overrightarrow{M}}{R}\, dV.$$

Since M is uniform here, the second term vanishes. In addition, the first term vanishes on the flat end faces. Thus A only depends on the surface contributions around the sides of the cylinder. We assume the sources for the potential are azimuthally directed Amperian currents with current density

$$\begin{aligned} \overrightarrow{K}_a &= \overrightarrow{M} \times \hat{n} \\ &= M\,\hat{\phi}. \end{aligned} \tag{9.1}$$

Thus the field in a bar magnet is analogous to the field in a solenoid, where the Amperian currents here take the place of the conduction currents in a solenoid. The magnetic flux density in the axial direction is then given by Equation 7.32

https://doi.org/10.1017/9781009291156.010 Published online by Cambridge University Press

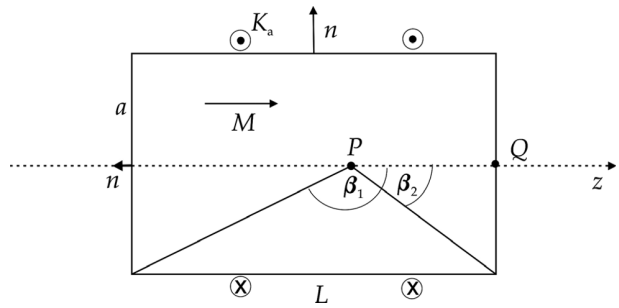

Figure 9.1 Bar magnet.

$$B_z(0,z) = \frac{\mu_0 nI}{2}\,(\cos\beta_2 - \cos\beta_1),$$

where β_i are the angles from the observation point along z to the two outer edges at the ends of the cylinder. Making the substitution $K_a = n\,I$, we get

$$\begin{aligned} B &= \frac{\mu_0 K_a}{2}\,(\cos\beta_2 - \cos\beta_1) \\ &= \frac{\mu_0 M}{2}\,(\cos\beta_2 - \cos\beta_1) \\ &= \frac{B_R}{2}\,(\cos\beta_2 - \cos\beta_1), \end{aligned} \tag{9.2}$$

where B_R is the remanent field for the permanent magnet. For a point P inside the magnet, $\cos\beta_1 < 0$ and $\cos\beta_2 > 0$. Thus B points along the positive z direction. From Gauss's law for a pillbox on one of the end faces, B must also be directed along $+z$ outside the magnet. We can find the magnetic intensity H from

$$\mu_0 H = B - \mu_0 M.$$

Thus [2]

$$\begin{aligned} H_P &= \frac{K_a}{2}\,(\cos\beta_2 - \cos\beta_1) - K_a \\ &= \frac{K_a}{2}\,(\cos\beta_2 - \cos\beta_1 - 2). \end{aligned} \tag{9.3}$$

Since the two cosine terms are both smaller than one, this expression is negative. Thus H inside the magnet points in the opposite direction from M and B.

Now let us consider the situation at the point Q on the end face of the magnet. In this case $\cos\beta_2 = 0$ and

https://doi.org/10.1017/9781009291156.010 Published online by Cambridge University Press

$$B_Q = -\frac{\mu_0 K_a}{2}\cos\beta_1. \tag{9.4}$$

On the inside surface of the end face, we find from Equation 9.3 that

$$H_Q^{in} = -\frac{K_a}{2}(\cos\beta_1 + 2),$$

which points along $-z$. On the outer surface of the end face, $M = 0$ and we find from Equation 9.4 that

$$H_Q^{out} = -\frac{K_a}{2}\cos\beta_1,$$

which points along $+z$. The behavior for H is similar to the case of the electric field from a surface distribution of charge. It is sometimes convenient when modeling bar magnets to assume that the end faces contain a distribution of fictitious magnetic charges or "poles." In terms of magnetic charges, we can express the surface and volume charge densities as [3]

$$\begin{aligned}\sigma_m &= \overrightarrow{M}\cdot\hat{n}\\ \rho_m &= -\nabla\cdot\overrightarrow{M}\end{aligned} \tag{9.5}$$

and the scalar potential as

$$V_m = \frac{1}{4\pi}\int\frac{\sigma_m}{R}\,dS + \frac{1}{4\pi}\int\frac{\rho_m}{R}\,dV. \tag{9.6}$$

Thus in a bar magnet, we can assume that B comes from the Amperian currents flowing azimuthally around the cylinder and that H comes from magnetic charges on the flat end faces. In a real bar magnet, M is typically weaker near the end faces than it is in the central region. In this case, there will also be contributions to the field from the volume integrals above.

Consider a bar magnet with radius a that is much smaller than its length L. This is sometimes referred to as a "magnetic needle."[4] We look at the field on the axis outside the magnet at location z. We have

$$\cos\beta_2 = -\left\{1 + \left(\frac{a}{z - L/2}\right)^2\right\}^{-1/2}.$$

For $a \ll L$,

$$\cos\beta_2 \simeq -1 + \frac{1}{2}\left(\frac{a}{z - L/2}\right)^2$$

https://doi.org/10.1017/9781009291156.010 Published online by Cambridge University Press

and we have a similar expression for cos β_1 with $L \rightarrow -L$. Then from Equation 9.2,

$$B(z) = \frac{\mu_0 M\, a^2}{4(z - L/2)^2} - \frac{\mu_0 M\, a^2}{4(z + L/2)^2}.$$

If we define the strength of the magnetic charge as

$$q_m = \pi a^2\, M, \tag{9.7}$$

we can write the magnetic intensity as

$$H(z) = \frac{q_m}{4\pi(z - L/2)^2} - \frac{q_m}{4\pi(z + L/2)^2}.$$

We interpret this as the field due to a positive magnetic charge at face 2 and a negative charge at face 1. The field strength falls off like the inverse square distance from the charge.

9.2 Magnetic circuit energized by a permanent magnet

Consider the arrangement shown in Figure 9.2, where a pair of permanent magnets surround an open gap on one side and are connected by an iron path on the other.[5] We know from the Ampère law that

$$\oint \vec{H} \cdot \vec{dl} = 0$$

around the circuit since there are no conduction currents. Assuming the gap is small and that the leakage flux is negligible, this gives

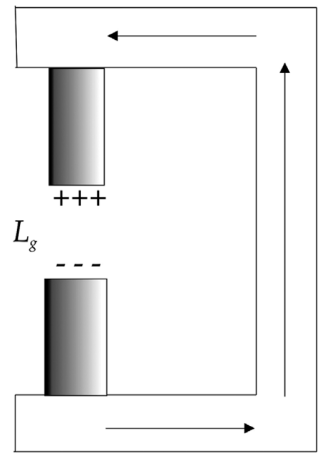

Figure 9.2 Magnetic circuit containing permanent magnets.

https://doi.org/10.1017/9781009291156.010 Published online by Cambridge University Press

$$H_g L_g - H_m L_m + H_i L_i = 0,$$

where the subscripts *g, m*, and *i* refer to gap, magnet, and iron. The quantity $H_m L_m$ takes the place of NI in magnetic circuits powered by conductors. Neglecting leakage, the flux is constant around the loop, so we have

$$\Phi_B = B_i A_i = B_g A_g = B_m A_m,$$

where A is the cross-sectional area. Combining these equations, we have

$$\begin{aligned} H_m L_m &= B_g A_g \left[\frac{H_g L_g}{B_g A_g} + \frac{H_i L_i}{B_g A_g} \right] \\ &= B_m A_m \left[\frac{L_g}{\mu_0 A_g} + \frac{L_i}{\mu A_i} \right] \\ &= \Phi_B \, R, \end{aligned} \tag{9.8}$$

where the series reluctance is

$$R = \frac{L_g}{\mu_0 A_g} + \frac{L_i}{\mu A_i}.$$

Equation 9.8 is analogous to Ohm's law with $H_m L_m$ corresponding to the applied voltage.

The magnetic energy stored in the gap is

$$\begin{aligned} W_g &= \tfrac{1}{2} \, \mu_0 B_g^2 A_g L_g \\ &= \tfrac{1}{2} \; H_g L_g B_g A_g. \end{aligned}$$

Since $\mu \gg \mu_0$, we can neglect the reluctance through the iron. Then

$$H_m L_m \simeq H_g L_g$$

and we can write

$$W_g \simeq \tfrac{1}{2} \, B_m H_m \, A_m L_m. \tag{9.9}$$

Thus the stored energy in the gap is proportional to the *BH* product and the volume of the permanent magnet.

Since B and H point in opposite directions, permanent magnets operate in the second quadrant of the hysteresis curve. To maximize the energy stored in the gap, it is desirable to operate at a point where the *BH* product is maximum. Rewriting Equation 9.8 as

https://doi.org/10.1017/9781009291156.010 Published online by Cambridge University Press

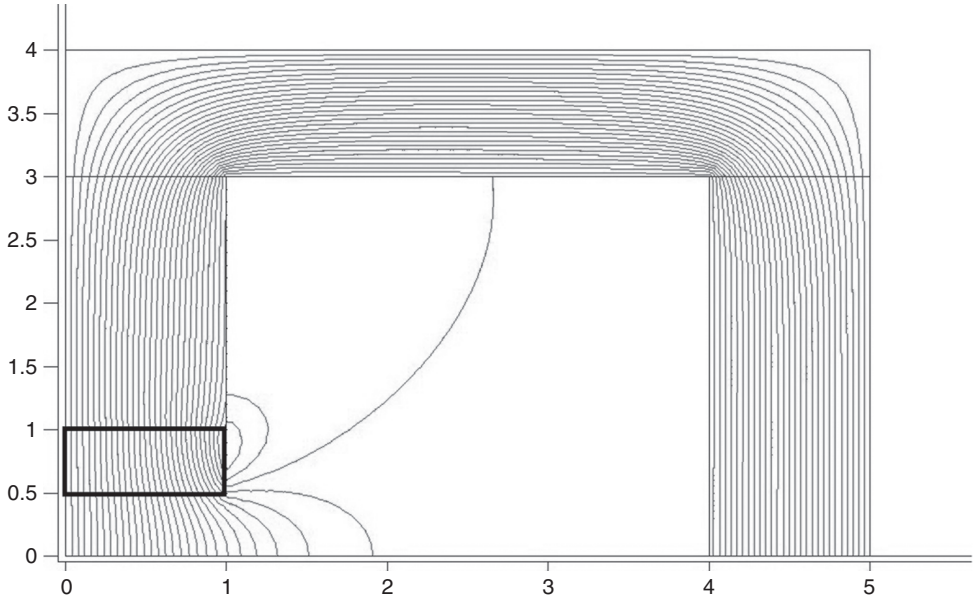

Figure 9.3 POISSON model of a magnetic circuit energized by a pair of permanent magnets.

$$\frac{B_m}{H_m} = \frac{L_m}{A_m R},$$

the quantities on the right-hand side can be adjusted to get the *B-H* "load line" for the magnetic circuit to pass through the point where the *BH* product is maximum.

Figure 9.3 shows a simple POISSON model[1] of a magnetic circuit energized by a pair of permanent magnets. The figure shows one quarter of a symmetric circuit. The *x* and *y* axes are symmetry planes in this figure. The use of a 2D program such as POISSON assumes that the configuration is uniform over a large distance in the third dimension (into the figure).

The permanent magnet material is located in the rectangle near the origin. The magnetization was oriented in the vertical direction. Considerable field fringing is evident in the air gap for this simple geometry. The amount of fringing depends strongly on the type of permanent magnet material that is used.[1]

9.3 Material properties

Characteristic properties of some permanent magnet materials are given in Table 9.1. Alnico is an alloy of iron with aluminum, nickel, and cobalt. It has

[1] The calculation was actually made with the PANDIRA program in the POISSON distribution.

https://doi.org/10.1017/9781009291156.010 Published online by Cambridge University Press

Table 9.1 *Properties of permanent magnet materials [6, 7]*

	B_R **[T]**	H_C **[kOe]**[1]	H_{Ci} **[kOe]**	$\boldsymbol{BH}_{\mathbf{max}}$ **[MG Oe]**
Alnico	0.83–1.25	0.6–6.4	0.6 – 1.9	1.4–5.5
Ceramic ferrite	0.22–0.39	1.9–3.2	2.5–3.3	1–3.6
SmCo	0.81–1.15	7.2–10.6	9–18	16–32
NdFeB	0.98–1.35	7.5–12.8	8–26	24–45

[1] 1 Oe = 1 10^{-4} T/ μ_0.

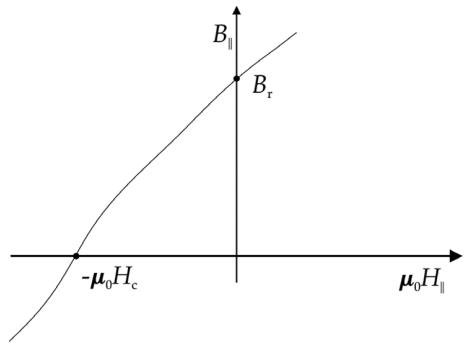

Figure 9.4 Second quadrant of the hysteresis curve.

a high remanent field but is easily demagnetized and has a large leakage flux.[1] Ferrite contains iron oxides (Fe_2O_3). It has a low B_R, but it is a cheap material. Ceramic ferrites are compounds of barium or strontium ferrite. Samarium and neodymium are rare earth elements.[8] They have large values of $(BH)_{\max}$, can produce a large field from a compact magnet, are very resistant to demagnification, and have small leakage flux.

9.4 Model for rare earth materials

Usually there is some direction in a crystalline material along which the moments in the material tend to align. This is referred to as the "easy" magnetization direction. A permanent magnet can be produced so that the maximum magnetization is along some desired direction. A useful model has been developed for describing the magnetic properties of rare earth materials.[1, 9] Figure 9.4 shows the second quadrant of a typical hysteresis curve for the easy direction. It is a good approximation to assume the relative permeability in this region is equal to 1, so we have the relation

$$B_R \simeq \mu_0 H_C.$$

https://doi.org/10.1017/9781009291156.010 Published online by Cambridge University Press

In this case, the fields from assemblies of blocks can be linearly superimposed. If the magnetization is anisotropic, the relation between B and H can be written as

$$\begin{aligned} B_{\parallel} &= \mu_{\parallel} H_{\parallel} + B_R \\ B_{\perp} &= \mu_{\perp} H_{\perp}, \end{aligned} \tag{9.10}$$

where $\parallel$ refers to the easy direction in the material and $\perp$ refers to the direction perpendicular to it. For convenience, we define the *reluctivity* $\gamma = 1/\mu$. Then from Equation 9.10, we have

$$\begin{aligned} H_{\parallel} &= \gamma_{\parallel} B_{\parallel} - \frac{B_R}{\mu_{\parallel}} \\ &\simeq \gamma_{\parallel} B_{\parallel} - H_C. \end{aligned} \tag{9.11}$$

These equations can be combined into the vector relations

$$\vec{B} = \mu_{\parallel} \vec{H}_{\parallel} + \mu_{\perp} \vec{H}_{\perp} + \vec{B}_R \tag{9.12}$$

and

$$\vec{H} = \gamma_{\parallel} \vec{B}_{\parallel} + \gamma_{\perp} \vec{B}_{\perp} - \vec{H}_C. \tag{9.13}$$

The vectors B_R and H_C are directed in opposite directions along the easy axis. Taking the divergence of Equation 9.12, we find that

$$\nabla \cdot (\mu_{\parallel} \vec{H}_{\parallel} + \mu_{\perp} \vec{H}_{\perp}) = -\nabla \cdot \vec{B}_R \equiv \rho_m, \tag{9.14}$$

which relates H to the density of magnetic charges. Taking the curl of Equation 9.13 in a region with no conduction currents, we get

$$\nabla \times (\gamma_{\parallel} \vec{B}_{\parallel} + \gamma_{\perp} \vec{B}_{\perp}) = \nabla \times \vec{H}_C \equiv \vec{J_m}, \tag{9.15}$$

which relates B to the Amperian currents. Thus the material can be treated magnetically as vacuum together with either a charge density $-\nabla \cdot \vec{B}_R$ or a current density $\nabla \times \vec{H}_C$. For homogeneous materials, these charges or currents vanish everywhere except on the surface.

The scalar potential for the permanent magnet material can be written as

$$\begin{aligned} \mu_0 V_m &= \frac{1}{4\pi} \int \frac{\rho_m}{R} \, dV \\ &= \frac{1}{4\pi} \int \frac{(-\nabla \cdot \vec{B}_R)}{R} \, dV, \end{aligned} \tag{9.16}$$

https://doi.org/10.1017/9781009291156.010 Published online by Cambridge University Press

where R is the distance between the source point and the field point. If the material is inhomogeneous, we can define $G = 1/R$ and make use of Equation B.3

$$\nabla\cdot(G\overrightarrow{B}_R) = G\,\nabla\cdot\overrightarrow{B}_R + \overrightarrow{B}_R\cdot\nabla G$$

to write Equation 9.16 in the form

$$\mu_0 V_m = -\frac{1}{4\pi}\int\left[\nabla\cdot(G\overrightarrow{B}_R) - \overrightarrow{B}_R\cdot\nabla G\right]\,dV.$$

Using the divergence theorem on the first part of the integrand,

$$\int\nabla\cdot(G\overrightarrow{B}_R)\,dV = \int G\overrightarrow{B}_R\cdot\hat{n}\,dS = 0,$$

which vanishes because we can choose the surface to lie outside the material where $B_R = 0$. We also have

$$\nabla G = -\frac{\overrightarrow{R}}{R^3}.$$

Thus the scalar potential for inhomogeneous material is

$$\mu_0 V_m = \frac{1}{4\pi}\int\frac{\overrightarrow{B}_R\cdot\overrightarrow{R}}{R^3}\,dV. \tag{9.17}$$

For homogeneous material, we can use the divergence theorem in Equation 9.16 and find that

$$\begin{aligned}\mu_0 V_m &= -\frac{1}{4\pi}\int\frac{\overrightarrow{B}_R\cdot\hat{n}}{R}\,dS \\ &= -\frac{\overrightarrow{B}_R}{4\pi}\cdot\int\frac{\hat{n}}{R}\,dS,\end{aligned} \tag{9.18}$$

where the final integral only involves geometric quantities.

9.5 Rare earth model in two dimensions

If the permanent magnet pieces are uniform over a long distance in the z direction and the magnetization does not have a component along z, then it is possible to make a two-dimensional approximation of the fields.[9] From Equation 5.40, the field at the observation point z_o is

https://doi.org/10.1017/9781009291156.010 Published online by Cambridge University Press

$$B^*(z_o) = \frac{\mu_0}{2\pi i}\iint \frac{\sigma}{z_o - z}\, dx\, dy. \tag{9.19}$$

We assume the remanent field can have both x and y components

$$B_R = B_{Rx} + i\, B_{Ry}.$$

From the curl $B = \mu_0\, J$ equation, we have

$$\partial_x B_{Ry} - \partial_y B_{Rx} = \mu_0\, \sigma.$$

Substituting back into Equation 9.19, we get

$$B^*(z_o) = \frac{1}{2\pi i}[\mathbb{I}_1 - \mathbb{I}_2], \tag{9.20}$$

where

$$\mathbb{I}_1 = \iint \frac{\partial_x B_{Ry}}{z_o - x - i\, y}\, dx\, dy$$
$$\mathbb{I}_2 = \iint \frac{\partial_y B_{Rx}}{z_o - x - i\, y}\, dx\, dy.$$

Considering the first integral, we integrate over x by parts with

$$u = \frac{1}{z_o - x - i\, y}$$
$$dv = \partial_x B_{Ry}\, dx,$$

which gives

$$\mathbb{I}_1 = \int \left[\frac{B_{R\,y}}{z_o - x - i\, y} - \int \frac{B_{R\,y}}{(z_o - x - i\, y)^2}\, dx \right] dy$$
$$= \oint \frac{B_{R\,y}}{z_o - x - i\, y}\, dy - \iint \frac{B_{R\,y}}{(z_o - x - i\, y)^2}\, dx\, dy.$$

The first term vanishes for a line integral evaluated outside the material where $B_R = 0$. Thus we have

$$\mathbb{I}_1 = -\iint \frac{B_{R\,y}}{(z_o - x - i\, y)^2}\, dx\, dy.$$

https://doi.org/10.1017/9781009291156.010 Published online by Cambridge University Press

For the integral $\mathbb{I}_2$, we integrate over y by parts to find

$$\mathbb{I}_2 = -i \iint \frac{B_{R\,x}}{(z_o - x - i\,y)^2}\; dx\, dy.$$

Substituting back into Equation 9.20, we find that [9]

$$B^*(z_o) = \frac{1}{2\pi} \iint \frac{B_R}{(z_o - z)^2}\; dx\, dy. \tag{9.21}$$

If the material is homogeneous,

$$B^*(z_o) = \frac{B_R}{2\pi} \iint \frac{1}{(z_o - z)^2}\; dx\, dy$$

we can apply the complex Green's function, Equation 5.39, with

$$F = \frac{B_R}{2\pi}\; \frac{1}{z_o - z}.$$

The field for a homogeneous block can then be written in terms of the contour integral

$$B^*(z_o) = -\frac{B_R}{4\pi\, i} \oint \frac{dz^*}{z_o - z}. \tag{9.22}$$

It is also possible by direct integration to write this in the alternate forms [9]

$$\begin{aligned} B^*(z_o) &= -\frac{B_R}{2\pi\, i} \oint \frac{dx}{z_o - z} \\ &= \frac{B_R}{2\pi} \oint \frac{dy}{z_o - z}. \end{aligned} \tag{9.23}$$

9.6 Multipole expansion for continuously distributed material

We next consider the problem of assembling permanent magnet material to make a 2D multipole magnet.[9, 10] In a multipole magnet, we try to make some multipole order N as large as possible, while at the same time making all the other orders small. We will mainly be concerned here with the magnetic field inside the aperture of the magnet. The field in general is given by Equation 9.21. In order to study the multipole structure of the field, it is convenient to first expand the denominator in a power series. We start with

https://doi.org/10.1017/9781009291156.010 Published online by Cambridge University Press

$$\frac{1}{z_o - z} = \frac{-1}{z\left(1 - \frac{z_o}{z}\right)} = -\sum_{m=0}^{\infty} \frac{z_o^m}{z^{m+1}}.$$

If we let $n = m + 1$, then

$$\frac{1}{z_o - z} = -\sum_{n=1}^{\infty} \frac{z_o^{n-1}}{z^n}. \tag{9.24}$$

Taking the derivative with respect to z of both sides gives

$$\frac{1}{(z_o - z)^2} = \sum_{n=1}^{\infty} \frac{n\, z_o^{n-1}}{z^{n+1}}. \tag{9.25}$$

Substituting back into Equation 9.21, we have

$$B^*(z_o) = \frac{1}{2\pi} \sum_{n=1}^{\infty} n\, z_o^{n-1} \int \frac{B_R}{z^{n+1}}\, dS.$$

We identify the n^{th} multipole field contribution as

$$B_n = \frac{n}{2\pi} \int \frac{B_R}{z^{n+1}}\, dS, \tag{9.26}$$

so the field in the aperture has the multipole expansion

$$B^*(z_o) = \sum_{n=1}^{\infty} B_n\, z_o^{n-1}. \tag{9.27}$$

It is possible to express B_n as a contour integral by defining

$$F = -\frac{B_R}{2\pi}\, z^{-n}$$

in the Green's theorem in Equation 5.39, which gives

$$B_n = \frac{B_R}{4\pi\, i} \oint \frac{dz^*}{z^n}. \tag{9.28}$$

Now let us consider the design of an ideal multipole magnet. We use a polar coordinate system with $z = r\, e^{i\phi}$. We assume the material is located in an annular region between the radii r_1 and r_2. Assume that we have the freedom to specify the direction of the easy axis everywhere in the material. Let the easy axis in the material located at angle ϕ be rotated through an angle $\beta(\phi)$ with

https://doi.org/10.1017/9781009291156.010 Published online by Cambridge University Press

respect to its direction at $\phi = 0$. The contribution to the field from the material at the angle ϕ is

$$B_r(\phi) = e^{i\beta(\phi)}\, B_R(0).$$

From Equation 9.26, the multipole field contribution is

$$B_n = \frac{n}{2\pi} \iint \frac{B_R \exp\{i[\beta(\phi) - (n+1)\phi]\}}{r^{n+1}}\; r\, d\phi\, dr. \tag{9.29}$$

The first term in the square brackets comes from the easy axis distribution and the second term comes from the azimuthal dependence in z^{n+1} in Equation 9.25. We can make the multipole as large as possible by making the quantity in square brackets equal to 0. This determines the constraint on the easy axis angles

$$\beta(\phi) = (n+1)\;\phi. \tag{9.30}$$

Multipole fields in the aperture can be produced by choosing n to be a positive integer N. For example, $N = 1$ produces a uniform dipole field in the aperture with no field outside the permanent magnet ring. Choosing n to be a negative integer on the other hand, produces a field outside the ring and no field in the aperture.[11] For example, $n = -1$ produces a dipole field outside the ring. Further control over the field can be obtained by surrounding the permanent magnet ring with an additional soft-iron ring.[11]

Confining our attention to $2N$-multipole fields inside the aperture, setting $n = N$ in Equation 9.30 and substituting into Equation 9.29 we find

$$B_n = \frac{n\, B_R}{2\pi} \int_{r_1}^{r_2} \frac{1}{r^n}\; \mathbb{I}\, dr,$$

where

$$\begin{aligned} \mathbb{I} &= \int_0^{2\pi} e^{i\,(N-n)\phi}\, d\phi \\ &= \begin{cases} 2\pi & \text{for } n = N \\ 0 & \text{for } n \neq N. \end{cases} \end{aligned}$$

For a dipole assembly, $N = 1$, and we have

$$B_1 = B_R \ln\left(\frac{r_2}{r_1}\right), \tag{9.31}$$

https://doi.org/10.1017/9781009291156.010 Published online by Cambridge University Press

while for higher order multipoles, $N \geq 2$, we get

$$B_N = N\,B_R \int_{r_1}^{r_2} \frac{dr}{r^N} = \frac{N\,B_R}{N-1}\,\frac{1}{r_1^{N-1}}\left[1 - \left(\frac{r_1}{r_2}\right)^{N-1}\right]. \tag{9.32}$$

The $2N$-multipole field at the point z_o is given by

$$B^*(z_o) = B_N\, z_o^{N-1}.$$

9.7 Segmented multipole magnet assemblies

In practical terms, the continuous distribution of easy axis directions discussed in the previous section can only be approximated by using a finite number of magnetized blocks. As a result, the strength of the desired multipole is reduced and unwanted multipole orders are introduced.

Assume that the multipole magnet is constructed from M geometrically identical rare earth trapezoidal blocks.[9] Each block is separated from its nearest neighbor by the angle $2\pi/M$ around the z axis. In each block, the easy axis direction is chosen to approximate the ideal angle given in Equation 9.30. The direction of the easy axis inside a block is made to rotate by the angle $(N+1)\,2\pi/M$ from a given block to its following neighbor. For example, Figure 9.5 shows a dipole magnet ($N = 1$) made up of $M = 8$ rare earth blocks. In this assembly, neighboring blocks are

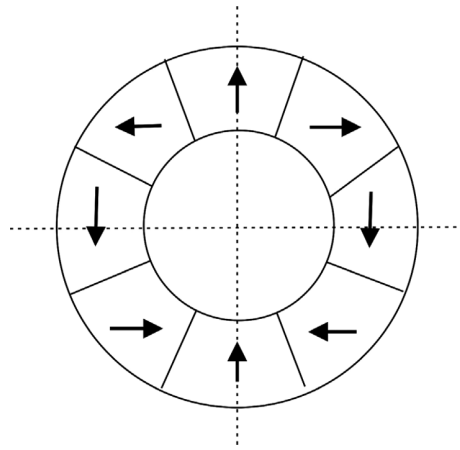

Figure 9.5 Dipole magnet made up from an assembly of trapezoidal-shaped permanent magnets.

https://doi.org/10.1017/9781009291156.010 Published online by Cambridge University Press

separated geometrically by the angle $\pi/4$ and the easy axis rotates by $\pi/2$ from block to block.

Let C_n be the contribution to the multipole B_n for some reference block. Then the contribution of block m to B_n is

$$C_n \exp\left\{ i\, m \frac{2\pi}{M}\ (N+1) \right\}\ \exp\left\{ -i\, m \frac{2\pi}{M}\ (n+1) \right\},$$

where the first exponential comes from the rotation of the easy axis and the second exponential comes from the definition of B_n. The sum of all M blocks gives

$$B_n = C_n \sum_{m=0}^{M-1} \exp\left\{ i\, 2\pi m \frac{N-n}{M} \right\},$$

where $m = 0$ refers to the reference block. If the quantity $(N-n)/M$ is a positive or negative integer, then by writing the exponential in terms of cosines and sines, we see that the value of the sum is M. If $(N-n)/M$ is not an integer, then the value of the sum is zero.[9] Thus we have from Equation 9.27

$$B^*(z_o) = M \sum_{v=0}^{\infty} C_n\, z_o^{N-1}, \tag{9.33}$$

where v is an index to the set of allowed multipoles. The multipole order that corresponds to a given v is given by [9]

$$n = N + vM. \tag{9.34}$$

Next we turn to finding the reference multipole C_n. Substituting the series expansion Equation 9.24 into the contour integral 9.23, we find we can express C_n as

$$C_n = \frac{B_R}{2\pi\, i} \oint \frac{dx}{z^n}.$$

Figure 9.6 shows the geometry of a trapezoidal block. Only the two segments marked 1 and 2 contribute to the contour integral. On path 1 we have

$$y = -x \tan\, \alpha,$$

where $\alpha = \pi/M$. On path 2 we have

$$y = x \tan\, \alpha.$$

https://doi.org/10.1017/9781009291156.010 Published online by Cambridge University Press

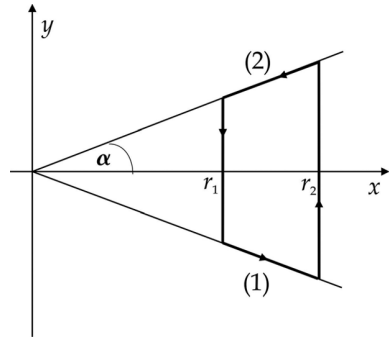

Figure 9.6 Trapezoidal block.

Thus the coefficient can be written as

$$C_n = \frac{B_R}{2\pi\, i}\left[\int_{r_1}^{r_2} \frac{dx}{(x - i\,x\,\tan\,\alpha)^n} + \int_{r_2}^{r_1} \frac{dx}{(x + i\,x\,\tan\,\alpha)^n}\right]$$

$$= \frac{B_R}{2\pi\, i}\left[\frac{1}{(1 - i\,\tan\,\alpha)^n}\int_{r_1}^{r_2} \frac{dx}{x^n} + \frac{1}{(1 + i\,\tan\,\alpha)^n}\int_{r_2}^{r_1} \frac{dx}{x^n}\right].$$

We can express

$$(1 \pm i\,\tan\,\alpha)^n = \frac{e^{\pm\, in\alpha}}{\cos^n\,\alpha}.$$

Performing the integrals and rearranging terms, we get

$$C_n = -\frac{B_R\,\cos^n\,\alpha}{2\pi\, i\,(n-1)r_1^{n-1}}\left[1 - \left(\frac{r_1}{r_2}\right)^{n-1}\right](e^{-in\alpha} - e^{in\alpha}).$$

Writing the exponential term as a sine function, we find that C_n for the trapezoidal block is

$$C_n = \frac{B_R}{\pi\,(n-1)r_1^{n-1}}\left[1 - \left(\frac{r_1}{r_2}\right)^{n-1}\right]\cos^n\,\alpha\,\sin\,n\alpha. \tag{9.35}$$

Substituting this back into Equation 9.33, we find that the field inside the aperture is given by

$$B^*(z_o) = B_R\sum_{\nu=0}^{\infty}\left(\frac{z_o}{r_1}\right)^{n-1}\frac{n}{n-1}\left[1 - \left(\frac{r_1}{r_2}\right)^{n-1}\right]K_n, \tag{9.36}$$

https://doi.org/10.1017/9781009291156.010 Published online by Cambridge University Press

Table 9.2 *Properties of a quadrupole magnet assembly*

M	K_2	$B_2(r_1)$ **[T]**	1st allowed harmonic [T]
4	0.32	0.454	$B_6(r_1) = -0.030$
8	0.77	1.095	$B_{10}(r_1) = -0.086$
12	0.89	1.270	$B_{14}(r_1) = -0.086$
16	0.94	1.336	$B_{18}(r_1) = -0.077$

where n is related to v by Equation 9.34 and we define the segmentation efficiency factor as [9]

$$K_n = \cos^n\left(\frac{\pi}{M}\right) \frac{\sin\left(\frac{n\pi}{M}\right)}{\frac{n\pi}{M}}. \tag{9.37}$$

The factor K_n measures how well a segmented magnet with M blocks approximates the idealized magnet with continuous variation of the easy axis that we described in the previous section.

Example 9.1: quadrupole magnet assembly

As an example, let us consider a quadrupole ($N = 2$) assembly made up of trapezoidal blocks. We assume $B_R = 0.95\ T$ and that $r_2/r_1 = 4$. We choose the observation point on the inner edge of the permanent magnet material, i.e., $z_o = r_1$. Table 9.2 shows some properties of the assembly as a function of the number of blocks M used around the circumference. The second column gives the segmentation efficiency factor for the quadrupole moment. We see that the efficiency increases quickly with the number of blocks used in the assembly. The third column gives the fundamental multipole contribution to the field. Already with 12 blocks, this contribution is almost 90% of the ideal unsegmented value. The last column shows the contribution to the field from the first allowed harmonic term. The strength of this term is ~7% of that for the fundamental.

Assemblies of permanent magnet blocks can be used to make many magnetic configurations, including dipoles, quadrupoles, sextupoles, solenoids, and periodic transverse fields.[1, 10]

References

[1] J. Bahrdt, *Permanent Magnets Including Undulators and Wigglers*, Proc. CERN Accelerator School on Magnets, Bruges, Belgium, June 2009, CERN-2010-004, p. 185.
[2] D. Tomboulian, *Electric and Magnetic Fields*, Harcourt, Brace & World, 1965, p. 240.
[3] L. Eyges, *The Classical Electromagnetic Field*, Dover, 1980, p. 139.

https://doi.org/10.1017/9781009291156.010 Published online by Cambridge University Press

[4] W. Smythe, *Static and Dynamic Electricity*, 2nd ed., McGraw-Hill, 1950, p. 434.
[5] P. Lorrain & D. Corson, *Electromagnetic Fields and Waves*, 2nd ed., Freeman, 1970, p. 409.
[6] *High Performance Permanent Magnets*, Magnet Sales and Manufacturing, Inc., Culver City, CA, 1993.
[7] A. Chao & M. Tigner, *Handbook of Accelerator Physics and Engineering*, World Scientific, 1999, p. 366.
[8] J. Becker, Permanent magnets, *Sci. Am*. 223:92, 1970.
[9] K. Halbach, Design of permanent multipole magnets with oriented rare earth cobalt material, *Nuc. Instr. Meth*. 169:1, 1980.
[10] A. Chao & M. Tigner, *op. cit*., p. 468.
[11] Q. Peng, S. McMurry & J. Coey, Cylindrical permanent magnet structures using images in an iron shield, *IEEE Trans. Mag*. 39:1983, 2003.